Journal of Chromatography A, 1223 (2012) 35–40

Contents lists available at SciVerse ScienceDirect

Journal of Chromatography A

journal homepage: www.elsevier.com/locate/chroma

Calculation of the geometrical three-point parameter constant appearing in the second order accurate effective medium theory expression for the B-term diffusion coefficient in fully porous and porous-shell random sphere packings

Sander Deridder, Gert Desmet*

Vrije Universiteit Brussel, Department of Chemical Engineering, Pleinlaan 2, 1050 Brussels, Belgium

ARTICLE INFO

Article history:
Received 29 July 2011
Received in revised form
23 November 2011
Accepted 1 December 2011
Available online 9 December 2011

Keywords:
B-term
Longitudinal diffusion
Peak parking
Effective medium theory
Three-point Parameter
Random sphere packing

ABSTRACT

Using computational fluid dynamics (CFD), the effective B-term diffusion constant γ_{eff} has been calculated for four different random sphere packings with different particle size distributions and packing geometries. Both fully porous and porous-shell sphere packings are considered. The obtained γ_{eff}-values have subsequently been used to determine the value of the three-point geometrical constant (ζ_2) appearing in the 2nd-order accurate effective medium theory expression for γ_{eff}. It was found that, whereas the 1st-order accurate effective medium theory expression is accurate to within 5% over most part of the retention factor range, the 2nd-order accurate expression is accurate to within 1% when calculated with the best-fit ζ_2-value. Depending on the exact microscopic geometry, the best-fit ζ_2-values typically lie in the range of 0.20–0.30, holding over the entire range of intra-particle diffusion coefficients typically encountered for small molecules ($0.1 \leq D_{pz}/D_m \leq 0.5$). These values are in agreement with the ζ_2-value proposed by Thovert et al. for the random packing they considered [1].

1. Introduction

The recently reported improvements in separation efficiency that can be obtained using porous-shell particles instead of fully porous particles [2–6] renews the interest in an accurate modeling of the B-term contribution to the band broadening in chromatographic columns. In a previous paper [7], our group has established effective medium theory [8–10] based expressions for the B-term diffusion in ordered sphere and cylinder packings, as well as in disordered cylinder packings. These are given by:

$$B = 2\gamma_{eff}(1+k') \tag{1}$$

$$\gamma_{eff} = \frac{1}{\varepsilon_T(1+k')}\frac{1+2\beta_1(1-\varepsilon_e)}{1-\beta_1(1-\varepsilon_e)} \tag{2}$$

$$\gamma_{eff} = \frac{1}{\varepsilon_T(1+k')}\frac{1+2\beta_1(1-\varepsilon_e)-\varepsilon_e\zeta_2\beta_1^2}{1+\beta_1(1-\varepsilon_e)-\varepsilon_e\zeta_2\beta_1^2} \tag{3}$$

$$\beta_1 = \frac{\alpha_{part}-1}{\alpha_{part}+2} \tag{4}$$

$$\alpha_{part} = \frac{\varepsilon_e k''}{1-\varepsilon_e}\frac{D_{part}}{D_m} = \frac{(1+k')\varepsilon_T-\varepsilon_e}{1-\varepsilon_e}\frac{D_{part}}{D_m} \tag{5}$$

In these equations, B is the longitudinal diffusion coefficient appearing in the B-term of the reduced plate height equation ($h_B = B/v_0$), γ_{eff} is the effective B-term diffusion constant, k' the phase retention factor, k'' the zone retention factor (related to the t_0-based retention factor k' via $k'' = (1+k')(\varepsilon_T/\varepsilon_e) - 1$), ε_T the total porosity, ε_e the external porosity, ζ_2 the three-point parameter, β_1 the polarizability constant, α_{part} the relative particle permeability and D_{part} and D_m the diffusion coefficient in the particles and mobile zone respectively.

These expressions were subsequently tested [11] for their ability to predict the effective diffusion coefficient in a variety of packing geometries with exact known intra- and inter-particle diffusion coefficients. For each geometry a wide range of different retention factors was considered, and the agreement was always very good. In most cases, the 1st-order approximation (Eq. (2)) was already accurate enough to approximate the true values within a few %. The excellent agreement also validated the adopted numerical calculation procedures. The study was however mostly limited to ordered spheres packings, and to packings where the spheres did not touch. The latter was due to the fact that the considered ordered sphere packings had an external porosity representative of those encountered in random packed bed columns (where typically $\varepsilon_e = 0.36$–0.40 [12]). Ordered packings with a face centered

* Corresponding author. Tel.: +32 2 629 32 51; fax: +32 2 629 32 48.
E-mail address: gedesmet@vub.ac.be (G. Desmet).

0021-9673/$ – see front matter © 2011 Elsevier B.V. All rights reserved.
doi:10.1016/j.chroma.2011.12.004

cubic or a body centered cubic arrangement however only reach their closest packed limit at resp. $\varepsilon_e = 0.26$ and $\varepsilon_e = 0.32$, so that the considered cases corresponded to a geometry where the spheres were "hanging" in space. This approach was justified because it was found that the effective diffusion was much more dependent on the value of the external porosity than on the actual sphere arrangement, so that it was more important to consider geometries with the correct external porosity than with the correct sphere position.

In the present paper, additional computational power was invoked to calculate the effective diffusion in more elaborate structures such as random sphere packings (i.e., with touching spheres). Both fully porous as well as porous-shell particles are considered. The main aim of the calculations was to investigate how well Eqs. (2) and (3) can predict the effective diffusion in these more complex cases. In the particular case of Eq. (3), the calculations are also used to determine the value of the three-point geometrical parameter (ζ_2) appearing in it. This was done for all different considered geometries.

2. Numerical methods and considered geometries

Fig. 1a–d represents the different considered random sphere packings. Each of the structures was first considered to consist of fully porous particles. Subsequently, also a series of porous-shell variants was considered. To characterize the thickness of the layer, the relative ratio (ρ) of the core diameter over the total diameter is being used, as is customary in the literature on porous-shell materials [2,5]. In the present study, the value of $\rho = 0.63$ was attributed to all porous-shell spheres, as this is a typical value found in the literature [13].

The first random sphere packing (Random I) was obtained by selecting 27 sphere diameters in such a way that the sphere diameters were distributed normally with a relative standard deviation $\sigma = 0.13$ (= standard deviation divided by the average sphere diameter), as an example of a commercial packing with a relatively broad PSD [14]. The spheres were subsequently randomly stacked such the resulting packing assumed an external porosity of 0.384 and fitted in a unit cell with a hexagonal cross-section, and with periodic boundaries (except for the top and bottom). The periodicity implies that an infinite space can be filled by stacking these unit cells, and that perfect spheres are created from the partial spheres on the periodic boundaries. The second random sphere packing (Random II) was obtained by randomly picking 29 spheres from a large batch of spheres with normally distributed diameters with a relative standard deviation of $\sigma = 0.13$. The spheres were subsequently randomly stacked such the resulting packing assumed an external porosity of 0.387 and fitted in a unit cell with a hexagonal cross-section, and with periodic boundaries (except for the top and bottom). The third random sphere packing was obtained by stacking 25 equally sized spheres in a unit cell with a square cross-section, and with periodic boundaries, in such a way that the resulting packing assumed an external porosity of 0.387. Finally, a fourth packing (Random IV) was generated using a numerical packing simulator (Macropac, Intelligensys [15]). This packing consisted out of 91 uniform spheres, and had a porosity of 0.387. Similar to the Random III-packing, it also had a square cross-section.

It was opted to consider packings with a similar external porosity ($\varepsilon = 0.385$), to rule out any effects induced by variations in packing density. The value of $\varepsilon = 0.385$ was selected as this lies near the average of the 0.36–0.4 range that is generally observed. [12,16].

To further characterize the packings, the average packing coordination number has been calculated according to the definition given in [17]. Random I and II have coordination number around 6 (resp.5.9 and 5.7), while Random III and IV have coordination number around 8 (resp. 8.2 and 8.1).

The effective diffusion in these packings has been numerically computed using the type peak parking simulations presented in [11]. The computational domains were meshed using

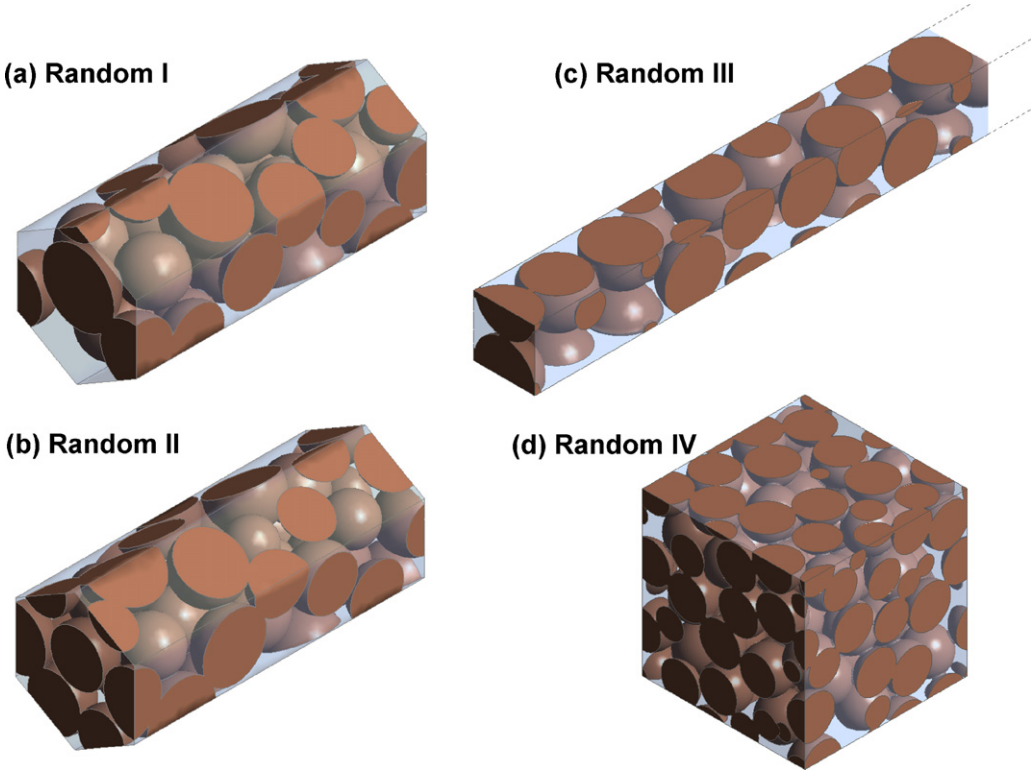

Fig. 1. (a–d) Unit cell containing randomly stacked spheres: (a) Random I, (b) Random II, (c) Random III and (d) Random IV.

1,500,000–4,000,000 tetrahedral cells. The maximum cell skewness never exceeded 0.90 and the average cell skewness was 0.2. Grid checks with half the amount of computational cells resulted in a maximum change of γ_{eff} of 0.11%. Periodic boundary conditions were applied to all boundaries, except for the top and bottom, for which constant zero-concentration conditions were applied. The mobile phase was given the properties of water and the meso-porous zone (either the fully porous particle or only the porous-shell layer) was attributed an internal porosity of 0.35 (as this is a typical literature value [18]). In the middle between top and bottom boundaries and parallel to them, a small region (with thickness of 7% of the average particle diameter) extending to the periodic boundaries of the flow domain was filled with a tracer liquid having the same physicochemical properties as the rest of the mobile phase. The tracer was attributed a diffusion coefficient D_m in the mobile zone and D_{pz} in the meso-porous zone in the particles. The tracer species was also subjected to a species equilibrium by means of a reversible chemical reaction that transforms the freely diffusing species A into a retained species A* via a forward and backward reaction rate combining into a given equilibrium constant $K_{A,pz}$ [19]. A fixed time stepping method was chosen to subsequently solve the diffusion equation using an implicit, segregated solution scheme with a second order implicit unsteady formulation. The resulting concentration field, which is a function of the time, was used to calculate γ_{eff} as described in [11].

For the sphere packings, two different values of the porous-zone diffusion coefficient were considered: one that is slightly higher than the highest D_{pz}-values observed [19] in state-of-the-art porous particles ($D_{pz} = 0.5 \cdot D_m$), and one ($D_{pz} = 0.1 \cdot D_m$) that is slightly smaller than the lower limit D_{pz}-value encountered in the same structures.

3. Results and discussion

Fig. 2a shows the computed γ_{eff}-values for the four considered random sphere packings represented in Fig. 1a–d ($D_{pz} = 0.5 \cdot D_m$-case), together with their best fit according to the Torquato-based expression (Eq. (3)), as well as the curve representing the more crude Maxwell-based expression (Eq. (2)). The latter is represented by the red curve. As can be noted, the four random cases lead to very similar γ_{eff}-values in the range of $2 < k'' < 6$ (see double x-axis to read out corresponding value of k'). The exact microscopic structure of the bed only becomes apparent for either very small or for large k''-values, where the respective γ_{eff}-curves clearly deviate from each other, albeit by no more than a few %. In these two ranges, the γ_{eff}-values can clearly also no longer be perfectly predicted by the simple Eq. (2). The higher order approximation (Eq. (3)), with a properly adapted ζ_2-constant depending on the exact microscopic geometry of the packing, clearly provides a much more accurate prediction. In the present study, the values of ζ_2 have been determined via a least-square fit of Eq. (3) to the computed CFD-data. The obtained values are given in Table 1. As a reference, the exact ζ_2-values that were determined by McPhedran and Milton [20] for the case of a perfectly ordered simple cubic (sc), face centered cubic (fcc) and body centered cubic (bcc) packing are given as well. As can be noted, the fitting is less accurate in the large k''-range. The origin of this poorer fit is discussed further on, in Figs. 3 and 4.

One of the virtues of the effective medium theory is that it also provides an elegant way to account for the presence of a solid core in a very simple way. This follows from the Hashin and Shtrikman-theory, according to which the D_{part}-value needed in Eq. (5) can be simply calculated by starting from the diffusion coefficient (D_{pz}) in the meso-porous zone of the particle (entire particle in case of fully porous particle or porous-shell layer in case of porous-shell particle) and multiply it with a fraction containing the dimensionless core diameter ρ ($\rho = d_{core}/d_p$):

$$D_{part} = \frac{2}{2 + \rho^3} D_{pz} \quad (6)$$

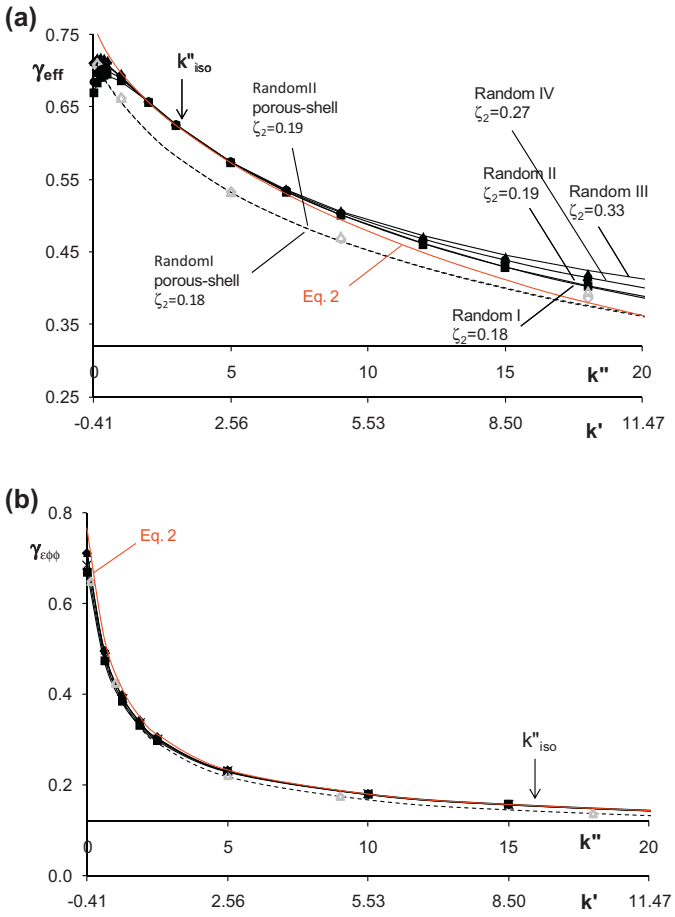

Fig. 2. Variation of γ_{eff} as a function of k'' for Random I (▲), Random II (◆), Random III (■), Random IV (*) and porous-shell Random I (◇) and II (△) as calculated from the simulation results and as calculated with: Eq. (2) (—), Eq. (3) with the best-fit ζ_2-values for Random I, II, III and IV (—) and Eq. (3) with the best-fit ζ_2-value for Random I and II in combination with Eq. (6) (....). (Porous-shell Random III and IV gave analogous results, data not shown) (a) $D_{pz}/D_m = 0.5$ and (b) $D_{pz}/D_m = 0.1$. The secondary axis (k'-axis) applies to the fully porous cases.

Table 1
Values of the 3-point parameter constant appearing in Eq. (3).

Geometry (random)	ζ_2	Geometry (perf. ordered)[a]	ζ_2
Random I ($\varepsilon_e = 0.384$)	0.20	Simple cubic ($\varepsilon_e = 0.386$)	0.44
Random II ($\varepsilon_e = 0.387$)	0.24	Body centered cubic ($\varepsilon_e = 0.386$)	0.091
Random III ($\varepsilon_e = 0.387$)	0.29	Face centered cubic ($\varepsilon_e = 0.386$)	0.071
Random IV ($\varepsilon_e = 0.387$)	0.27		
Random (taken from ref. [1], $\varepsilon_e = 0.386$)	0.31		

[a] Values taken from ref. [20]

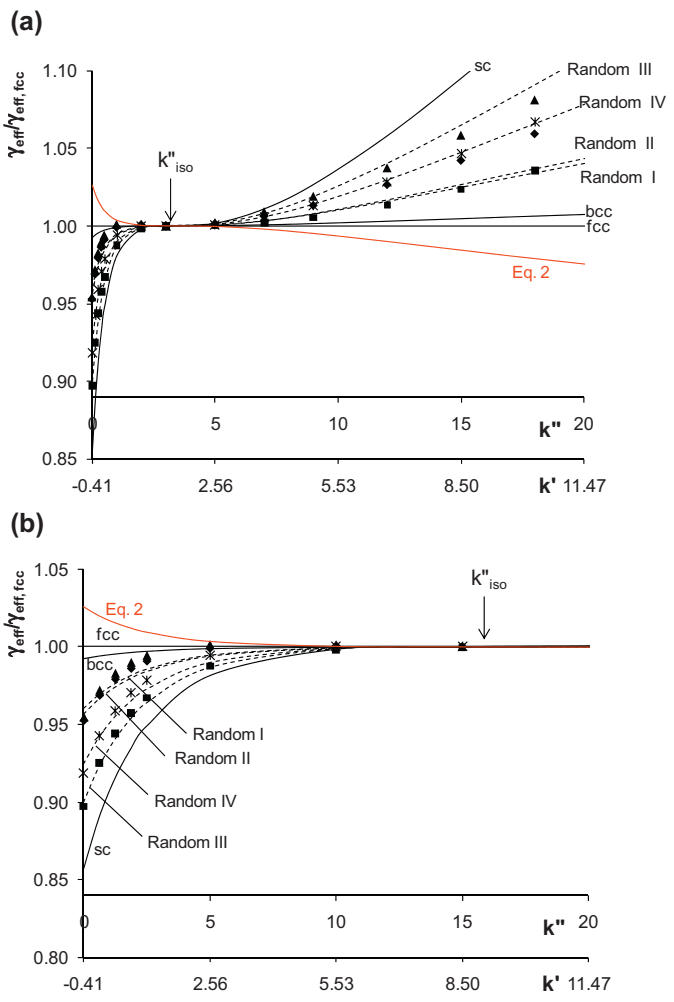

Fig. 3. Variation of $\gamma_{eff}/\gamma_{eff,fcc}$ (γ_{eff} divided by γ_{eff} predicted by Eq. (3) for the case of an fcc packing) as a function of k'' for Random I (▲), Random II (♦), Random III (■) and Random IV (*) as calculated from the simulation results and as calculated with: Eq. (2) (—), Eq. (3) (—) with ζ_2 as predicted in [20] for an fcc-, bcc- and sc-packing and Eq. (3) with the best-fit ζ_2-values for Random I, II and III (....). (a) $D_{pz}/D_m = 0.5$ and (b) $D_{pz}/D_m = 0.1$. The secondary axis (k'-axis) applies to the fully porous cases.

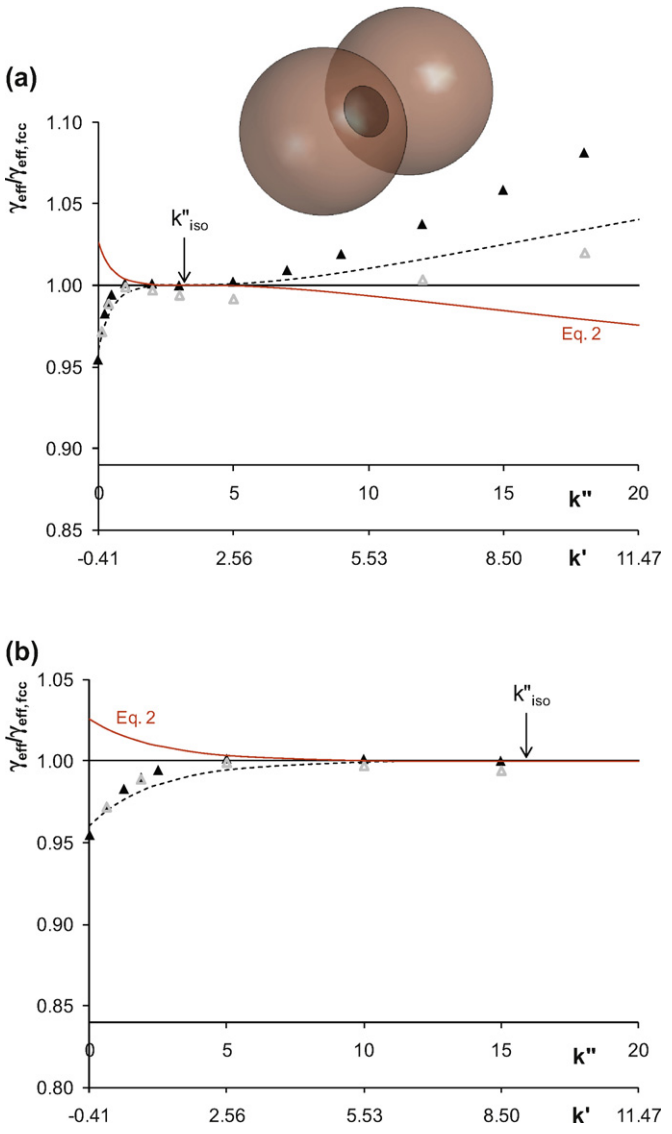

Fig. 4. Variation of $\gamma_{eff}/\gamma_{eff,fcc}$ (γ_{eff} divided by γ_{eff} predicted by Eq. (3) for the case of an fcc packing) as a function of k'' for Random I and Random I (▲) with blocked diffusion through the particle contact zones (◇) as calculated from the simulation results and as calculated with: Eq. (2) (—), Eq. (3) with ζ_2 as predicted in [20] for an fcc – packing (—) and Eq. (3) with the best-fit ζ_2-values for Random I (....). (a) $D_{pz}/D_m = 0.5$ and (b) $D_{pz}/D_m = 0.1$ Inset: Two spheres with a blocked contact region (dark).

When $\rho = 0$ (fully porous particle), Eq. (6) returns the trivial result that $D_{part} = D_{pz}$. When $\rho = 0.63$ (presently considered porous-shell case), Eq. (6) returns $D_{part} = 0.89 \cdot D_{pz}$. Using the latter value, while keeping the same ζ_2-value as obtained by fitting the fully porous particle case, the resulting γ_{eff}-model curves can clearly fit the γ_{eff}-values computed for the porous-shell particle packings. This holds for both the $D_{pz}/D_m = 0.5$-case in Fig. 2a, as well as for the $D_{pz}/D_m = 0.1$-case represented in Fig. 2b. In the latter case, the four different random cases produce γ_{eff}-values that seem to fall much closer to each other. This holds as well for the fully porous as for the porous-shell case. This is essentially a visual effect, caused by the steeper decrease of the γ_{eff}-values, as a detailed zoom-in of the data (see Fig. 3 further on) shows that both D_{pz}/D_m-cases have a similar fitting accuracy.

In both the $D_{pz}/D_m = 0.5$ and the $D_{pz}/D_m = 0.1$-case, there is always a range of k''-values where γ_{eff} is insensitive to the actual packing geometry. An explanation for this observation has already been given in [7] for the case of ordered sphere packings and can now be generalized to any kind of packing. The observed insensitivity to the actual packing geometry in a given range of k''-values is due to the fact that, for that range of retention factors, the effective permeability of the particles (whose effective permeability is proportional to the product of internal diffusion coefficient and the particle-based retention factor) is of the same order as the permeability of the surrounding mobile phase liquid. As a consequence, it becomes irrelevant whether the species are diffusing through the particles or through the surrounding mobile phase, and the effective diffusion becomes insensitive to the geometrical arrangement of both zones. Mathematically, this is expressed by the fact that the relative permeability of the particle zone (represented by the relative permeability α_{part}, see Eq. (4)) becomes unity. This leads to the following expression for the critical zone and phase retention factor:

$$k''_{iso} = \frac{1 - \varepsilon_e}{\varepsilon_e} \frac{D_m}{D_{part}} \tag{7}$$

For the case of $D_{pz}/D_m = 0.5$, the critical k''-value for the fully porous particle case predicted by Eq. (7) is given by $k''_{iso} = 3.18$. This value indeed lies exactly in the range where the γ_{eff}-curves corresponding to the different geometries all perfectly coincide. This is

more clearly observed in Fig. 3, where the differences between the different γ_{eff}-curves are magnified by switching to a representation where the absolute γ_{eff}-values are divided by the γ_{eff}-values predicted by Eq. (4) in case of an fcc-packing (represented by the black, solid line).

When the intra-particle diffusion is smaller (cf. the $D_{pz}/D_m = 0.1$-case represented in Figs. 2b and 3b), the range where the geometry has nearly no effect on γ_{eff} shifts to higher values as k''_{iso} increases with a factor 5 compared to the $D_{pz}/D_m = 0.5$-case. In addition, the range of small k''-values where the microscopic detail of the packing has a significant effect on γ_{eff} is proportionally elongated, so that now the more simple Eq. (2) is clearly less accurate than the higher order Torquato-based variant (Eq. (3)) in the k''-region between 0 and 5 (or equivalently $0 < k' < 3$). Above $k'' = 5$, the effect of the microscopic structure of the bed on γ_{eff} again vanishes and the γ_{eff}-curves of the different considered geometries can all be perfectly predicted using the more simple Eq. (2).

Since a random packing can be conceived as a combination of the three basic ordered packing variants (sc, fcc and bcc), it is in full agreement with one's physical expectations to observe that the data for the four random packing cases represented in Fig. 3 lie within the range formed between the full line curve representing the pure sc-packing and the two full line curves representing the pure fcc- and bcc-packings. This is further confirmed by the fact that the best-fit ζ_2-values for the considered random sphere packings lie in the range formed between the pure sc-packing ($\zeta_2 = 0.44$) and the pure fcc- and bcc-packing (resp. $\zeta_2 = 0.071$ and $\zeta_2 = 0.091$). The best-fit ζ_2-values for the random sphere packings in the present study also lie close to the ζ_2-value of 0.31 proposed by Thovert et al. [1] for the random sphere packing they considered (see also Table 1). Obviously, the difference between the latter value and the values obtained in the present study is due to the fact that the result in [1] relates to a random packing with a different geometry.

Considering Random I and II have very similar properties (coordination number around 6 and packed with particles with a particle size distribution with $\sigma = 0.13$), while Random III and IV have different, but mutually also very similar properties (coordination number around 8 and with $\sigma = 0$), it is interesting to observe from Fig. 3a and b that the difference between the members of the same pair can be as large as the difference between the pairs (see right hand side of k''_{iso}-point in Fig. 3a). This suggests that it will be difficult to grasp the exact value of ζ_2 using just one or two general numbers, but that ζ_2 should be calculated by taking the exact position of each sphere into account if one is after the full precision.

It is also important to note that, in agreement with Eq. (6), only one ζ_2-value is needed to fit both the $D_{part}/D_m = 0.1$ and the $D_{part}/D_m = 0.5$-case, as well as the porous-shell and the fully porous particle case within a reasonable accuracy. This shows that the calculated ζ_2-parameter is a true geometrical parameter, and not just a fitting constant whose value depends on the diffusion properties of the particles. Eq. (6) follows directly from the coated-sphere solutions of the effective medium theory [7,11].

A general trend observed in Figs. 2 and 3 is that the agreement between the best-fit with Eq. (3) and the computed data is not perfect over the entire range of considered k''-values, as there clearly is always a region of deviation on the order of a few % between the computed data and the best-fit curve. To further improve the accuracy, one of the higher order accuracy expressions that can be derived from the effective medium theory [21] scheme could be used, introducing also a four-point parameter, a five-point parameter, etc. It is however believed that the accuracy offered by the presently considered second order-accurate expression, requiring only a three-point geometrical parameter, is more than sufficient, as typical experimental errors are anyhow on the order of 5–10% [19,22,23].

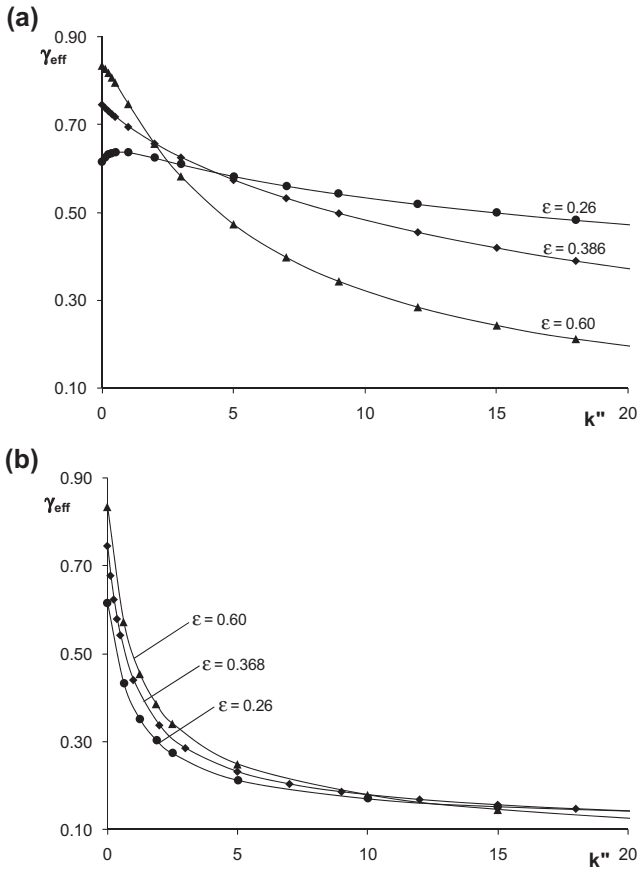

Fig. 5. Variation of computed γ_{eff}-data as a function of k'' for the fcc packing with external porosity $\varepsilon_e = 0.26$ (●), 0.386 (♦) and 0.6 (▲). Solid lines calculated using Eq. (3) with ζ_2 as predicted in [20] for an fcc-packing. (a) $D_{pz}/D_m = 0.5$ and (b) $D_{pz}/D_m = 0.1$.

It was also attempted to investigate why the presently considered random sphere packings deviate much more from the simple Maxwell-based expression (Eq. (2), see red curve) than the perfectly ordered packings considered in [11]. More specifically, it was investigated whether the deviation is due to the randomness itself or rather due to the fact that the spheres in the random packings are actually touching (whereas they are not when considering a fcc- and bcc-packing with the same $\varepsilon_e = 0.385$). A first indication in this respect, hinting at the importance of the sphere-to-sphere contact, is the position of the sc-curve in Fig. 3 (deviating most strongly from the red reference curve). For the considered porosity of $\varepsilon_e = 0.385$, the sc-packing corresponds to a case where the spheres are not only touching but are actually already overlapping. To gain more insight in this problem, a series of simulations was conducted on a random packing of spheres (Random I, see Fig. 1a) where the contact zone between two adjacent spheres was replaced by an impenetrable solid disk (see inset of Fig. 4) to block the diffusion flux through the contact zone. As can be noted (see open triangles added to Fig. 4), the blocking of the sphere-to-sphere contact has little or no influence in the range of very small k''-values. For larger k''-values on the other hand, the presence of the blocking disks leads to a significant reduction of γ_{eff}. These observations can readily be understood as follows. For small values of k'', the diffusion essentially occurs through the interstitial void space, as the majority of the species anyhow diffuse around the particles when the relative permeability of the particles is small (small k'' leads to small α_{part}, see Eq. (5)). As a consequence, the blocking of the sphere-to-sphere contact has little or no influence on the effective diffusion rate. For large values of k'', the opposite occurs, as in this case the majority of the species

diffuse through the particles, so that the sphere-to-sphere contacts become very important.

The observation is in line with the shortcomings of Eq. (3) already discussed by Torquato [21]. According to this work, Eq. (3) is essentially suited for dispersions of particles which do not form large clusters, whereas it becomes less accurate in the case of bicontinuous porous media. When the diffusive permeability of the spheres is large, packings of touching spheres indeed behave rather like a bicontinuous porous medium.

As a side note, practically less relevant but important to understand the dynamics of Eq. (3), Fig. 5 shows the effect of the external porosity on γ_{eff} for the case of the ordered fcc-packing. Comparing the spread of the curves with those observed in Fig. 2, it can be clearly observed that the value of the external porosity (ε_e) has a much stronger influence on the value of γ_{eff} than the microscopic details of the packing arrangement. The effect is more pronounced for the high $D_{\text{pz}}/D_{\text{m}}$-case than for the low $D_{\text{pz}}/D_{\text{m}}$-case, again due to the fact that in the latter case the γ_{eff}-curves decrease more steeply and are elongated in the direction of increasing k''-values.

Whereas the presently considered packings all had an external porosity of 0.385, it can be assessed from the general effective medium theory [21] that an increase of the porosity of about 0.015 (e.g., changing ε from 0.385 to 0.40) would lead to a decrease of ζ_2 of about 2.4%. For some typical sets of separation conditions, this would maximally change γ_{eff} by −1.0% ($k'' = 0$) to 2.3% ($k'' = 20$).

4. Conclusion

The B-term contribution to the band broadening in random packed beds of fully porous as well as porous-shell particles can be very closely approximated (to within 1 to 2% accuracy) over a broad range of retention factors and values of the porous zone diffusion coefficient using the 2nd-order accurate effective medium theory expression given by Eq. (3). The accuracy is significantly better than what can be obtained with the 1st-order accurate Maxwell expression (Eq. (2)). Eq. (3) contains a single geometrical tuning factor (the three-point parameter ζ_2) whose value needs to be determined via numerical calculations taking into account the microscopic details of the packing, as was done in the present study for a number of different examples. Since there are many different real packed bed configurations, each of these real packed beds will have to be described by a different zeta-value, at least if one would be after the ultimate prediction accuracy. In that case, the only way to find the true zeta-value consists of repeating the numerical calculations as in the present paper, but on an exact replica of the packing (if ever this would be available). If one is satisfied with a lower accuracy, which is certainly allowed when k'' is close to k''_{iso} (see Eq. (7)), the values calculated in the present study can be used as a first estimate. Typically, the ζ_2-parameter can be expected to lie in the range between 0.20 and 0.30 for a random packing of touching spheres, regardless whether the spheres are fully porous or only have a porous shell.

Eq. (3) becomes less accurate when both the intra-particle diffusion coefficient and k'' are large, i.e., when the relative permeability α_{part} is significantly larger than unity. In this case, the bicontinuous character of the packing becomes apparent, and it is well known from theory [21] that in this case Eq. (3) is less accurate.

References

[1] J.F. Thovert, I.C. Kim, S. Torquato, A. Acrivos, J. Appl. Phys. 67 (1990) 6088.
[2] A. Cavazzini, F. Gritti, K. Kaczmarski, N. Marchetti, G. Guiochon, Anal. Chem. 79 (2007) 5972.
[3] Y. Zhang, X. Wang, P. Mukherjee, P. Petersson, J. Chromatogr. A 1216 (2009) 4597.
[4] E. Oláh, S. Fekete, J. Fekete, K. Ganzler, J. Chromatogr. A 1217 (2010) 3642.
[5] F. Gritti, I. Leonardis, D. Shock, P. Stevenson, A. Shalliker, G. Guiochon, J. Chromatogr. A 1217 (2010) 1589.
[6] D. Guillarme, J. Ruta, S. Rudaz, J. Veuthey, Anal. Bioanal. Chem. 397 (2010) 1069.
[7] G. Desmet, S. Deridder, J. Chromatogr. A 1218 (2011) 32.
[8] M. Barrande, R. Bouchet, R. Denoyel, Anal. Chem. 79 (2007) 9115.
[9] F. Gritti, I. Leonardis, J. Abia, G. Guiochon, J. Chromatogr. A 1217 (2010) 3819.
[10] E.L. Cussler, Diffusion Mass Transfer in Fluid Systems, Cambridge University Press, Cambridge, 1984.
[11] S. Deridder, G. Desmet, J. Chromatogr. A 1218 (2011) 46.
[12] F.A.L. Dullien, Porous Media. Fluid Transport and Pore Structure, 2nd ed., Academic Press Inc., 1992.
[13] J.J. Kirkland, T.J. Langlois, J.J. DeStefano, Am. Lab. 39 (2007) 18.
[14] D. Cabooter, A. Fanigliulo, G. Bellazzi, B. Allieri, A. Rottigni, G. Desmet, J. Chromatogr. A 1217 (2009) 7074.
[15] A. Liekens, J. Billen, R. Sherant, H. Ritchie, J. Denayer, G. Desmet, J. Chromatogr. A 1218 (2011) 6654.
[16] D. Cabooter, J. Billen, H. Terryn, F. Lynen, P. Sandra, G.Desmet, J. Chromatogr. A 1178 (2008) 108.
[17] K. Lochmann, L. Oger, D. Stoyan, Solid State Sci. 8 (2006) 1397.
[18] A. Liekens, J. Denayer, G. Desmet, J. Chromatogr. A 1218 (2011) 4406.
[19] P. Gzil, N. Vervoort, G.V. Baron, G. Desmet, Anal. Chem. 75 (2003) 6244.
[20] R.C. McPhedran, G.W. Milton, Appl. Phys. A: Mater. 26 (1981) 207.
[21] S. Torquato, Random Heterogeneous Materials, Springer Science & Business Media, New York, 2002.
[22] L. Hong, A. Felinger, K. Kaczmarski, G. Guiochon, Chem. Eng. Sci. 59 (2004) 3399.
[23] K. Miyabe, N. Ando, G. Guiochon, J. Chromatogr. A 1216 (2009) 4377.